Heavily Boron Doped Diamond Powder: Synthesis and Rietveld Refinement

Igor P. Zibrov * and Vladimir P. Filonenko

Institute for High Pressure Physics RAS, Kaluzhskoe highway, Str. 14, Troitsk, Moscow 108840, Russia; filv@hppi.troitsk.ru

* Correspondence: zibrov@hppi.troitsk.ru; Tel.: +7495-8510738; Fax: +7495-8510012

Abstract: Boron-doped diamonds were synthesized by the reaction of an amorphous globular carbon powder (80%) with a powder of 1,7-di (oxymethyl)-M-carborane (20%) in a 'toroid'-type high-pressure chamber at a pressure of 8.0 GPa and temperature of 1700 °C. The structure was refined by the Rietveld method according to the X-ray powder diffraction data. It was shown that the unit cell parameters of these diamonds have two discrete quantities: around 3.570 Å for small concentrations of B (~1–1.5%) and around 3.578 Å for large concentrations of B (~2–3%). The concentration of the vacancies in the diamonds exceeds the concentration of boron atoms by 2–3 fold. This fact can play an important role in the formation of the structure and in determining the physical properties of diamonds.

1. Introduction

Diamond is a unique material that is used in various industrial areas, especially in electronics [1,2]. There is active investigation into the possibility of introducing different elements into the diamond lattice. This aims to complement the outstanding properties of diamonds, including high hardness, high thermal conductivity, and high chemical resistance to acids and alkalis, with new optical and electrical characteristics. Most natural and synthetic diamonds contain nitrogen, which makes them yellow. Nitrogen acts as a substitute for carbon in diamond, with a maximum concentration of about one percent (~10^{20} cm^{-3}). The content of larger atoms (Si, Ti, Ni, Ge, and P) in the diamond lattice is less than 0.01%. They form dopant–vacancy complexes with different luminescent characteristics [3,4]. As a rule, substituting atoms slightly increases the diamond unit cell parameter.

Boron is a neighbor of carbon in the periodic table although it is rarely found in natural diamonds. Several methods have been developed for producing boron-doped diamonds (BDD) with low electrical resistance, high mobility of charge carriers, and p-type conductivity. Large single crystals are synthesized at pressures of about 5 GPa [5]. In this case, the boron is in the molten metal through which the graphite recrystallization takes place. As the concentration of boron increases, the color of diamond changes from blue to black. Various methods of growing diamond films have also made it possible to produce single crystals with a boron content of >10^{20} cm^{-3} in the lattice [6]. The electrical conductivity of BDD is most often used for the manufacture of electrodes and sensors. Both CVD films and microcrystals are used for this purpose [7–9].

With an increase in the boron concentration, the conductivity of the diamond increases. If the content of boron is more than 1 wt %, the transition of the material to a superconductor can be observed at helium temperatures. The superconductivity of BDD was first discovered in 2004 with a polycrystalline sample synthesized from a mixture of graphite and boron carbide [10].

It is known that the unit cell parameter of the diamond increases with the substitution of carbon by boron. The maximum increase was recorded in [11,12]. As a result of the graphite–diamond phase transition, polycrystals with the unit cell parameters of 3.574–3.577 Å were formed, with the content of boron in these polycrystals being estimated at 3–4 wt %.

Despite the large number of results relating to the production and study of BDD, discussions about the concentration of boron and its role in superconductivity is ongoing. This is partly due to the fact that good-quality single crystals with a high content of boron have not yet been obtained.

The goal of this work was to synthesize microcrystals of diamonds with high boron content, with subsequent refinement of their structure.

2. Materials and Methods

The starting materials for the work were amorphous globular carbon powder with particle sizes of about 25 nm (80%) and powder of 1,7-di (oxymethyl)-M-carborane with the formula $HO-H_2C-CB_{10}H_{10}C-CH_2-OH$ (20%) (Aviabor, Dzerzhinsk, Russia). M-carborane decomposes at a high temperature to form active atomic boron. The powders were stirred in alcohol with application of ultrasound. The obtained mixture was pressed into pellets with the following dimensions: 3 mm in height and 5 mm in diameter. The thermobaric treatment of pellets was conducted in "toroid"-type high-pressure chambers. The scheme of the high-pressure chamber and the method were previously described in references [13,14]. The temperature in the chamber was calibrated using a W:W-Re thermocouple, with the accuracy of measurements estimated at ± 25 °C. The material was treated under the following conditions: P = 8.0 GPa, T = 1700 °C for 20 s (sample N1) and 30 s (sample N2).

Crystal morphology was studied using microscopes SEM JSM-6390 JEOL (JEOL Ltd., Tokyo, Japan) and TEM JEM-2100 JEOL (JEOL Ltd., Tokyo, Japan) with accelerating voltage of 200 kV.

Micro-Raman measurements were obtained at room temperature using the TriVista 555 triple grating spectrometer with a liquid-nitrogen-cooled CCD detector. The 488 nm line of the Ar^+ ion laser was used for excitation. To avoid overheating or burning out of the samples, the laser power was kept at a minimum (approximately 0.5 mW) and the $50\times$ objective (NA = 0.5) of Olympus BX51 microscope (Olympus, Tokyo, Japan) was used for laser focusing and the scattered light collection.

A Huber Imaging Plate Guinier camera G670 (Cu $K\alpha_1$ radiation, Huber Technology, Tutzing, Germany) was used for the phase analysis and data collection.

3. Results

The chemical interaction of amorphous globular nano-carbon with active boron leads to BDD crystallization with particle sizes of up to 5 μm in a few seconds. Phase analysis showed that both samples consist of three phases: two diamond D1 and D2 with different unit cell parameters and carbide B_4C. In this case, the diamond phases had unit cell parameters greater than that of a pure diamond (a = 3.567 Å, ICSD 76766), which is one of the indicators of a heavily BDD. This is well illustrated by the diffraction patterns in the region of the diamond peak (311) (Figure 1). Raman spectra of the obtained diamonds (Figure 2) also showed features that were characteristic of crystals with a high content of boron in the lattice. The characteristics and description of these features can be found in a previous study [15]. The difference in the spectra of Samples 1 and 2 is due to the different content of D1 and D2 (Tables 1 and 2). M-carborane contains 52.92% of boron and thus, the content of boron is 10.59% in the samples.

Diamond single crystals were formed during the thermobaric treatment of mixtures of nano-carbon with M-carborane, which have dimensions in the range of submicrons to several micrometers. The morphology of the crystals is shown in Figure 3.
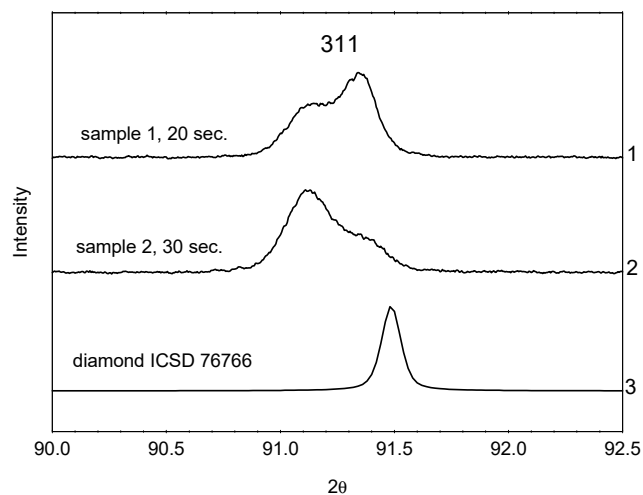
Figure 1. Diffraction patterns in the region of the diamond peak (311): 1—sample N1, 2—sample N2, 3—diamond ICSD 76766.
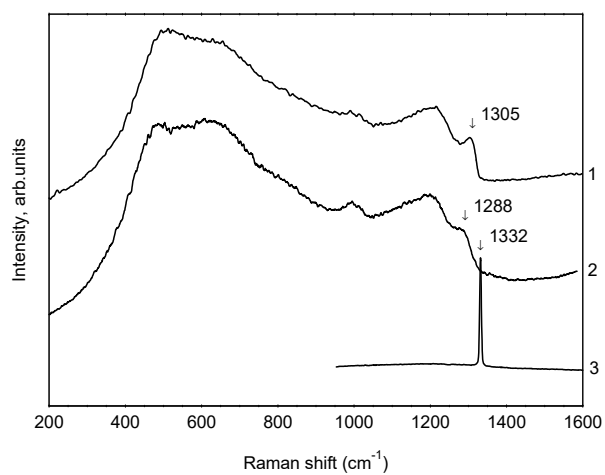

Figure 2. Raman spectra: 1—Sample N1; 2—Sample N2; 3—ordinary microdiamond.
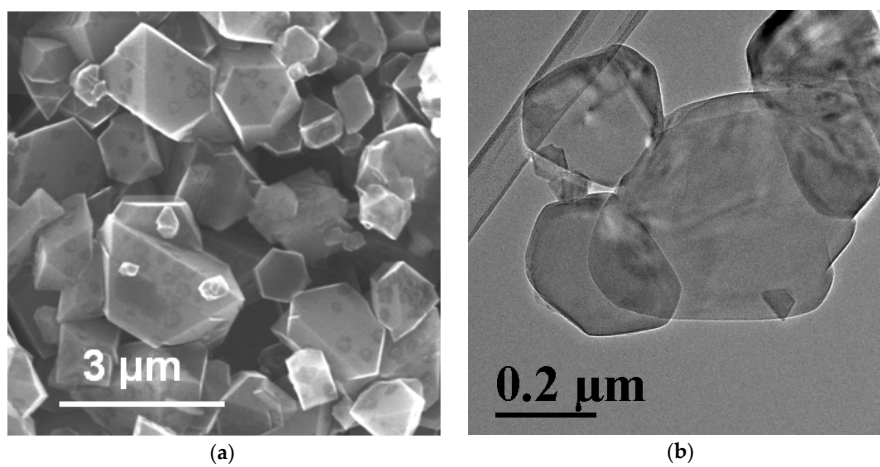

(**a**)   (**b**)

Figure 3. Morphology of boron doped diamond crystals. Synthesis from a mixture of globular nano-carbon and M-carborane. (**a**) SEM; (**b**) TEM.

Rietveld full-profile refinement was performed with the program GSAS [16,17]. The observed diffractometer data and the difference between the observed and calculated data are shown in Figures 4 and 5. The crystal data and structure refinement are shown in Tables 1 and 2. The unit cell parameters and the weight fraction in the mixture were refined for B_4C, while the atomic parameters were taken from [18].

We can calculate the content of boron in diamonds as we know the weight fraction of boron carbide in the sample (Tables 1 and 2). Boron carbide has a broad homogeneity region. When changing the composition of carbide from B_8C to B_4C, the parameters of the unit cell are significantly reduced. If we compare the unit cell volumes of boron carbide in Samples 1 and 2 (Tables 1 and 2) with the results obtained in [19], it can be concluded that the composition is B_4C. The boron concentration in the diamonds were calculated to be 1.93% and 1.51% for Samples 1 and 2, respectively. Obviously, the calculations are carried out under the assumption that all boron from M-carborane passes into diamonds and carbide.
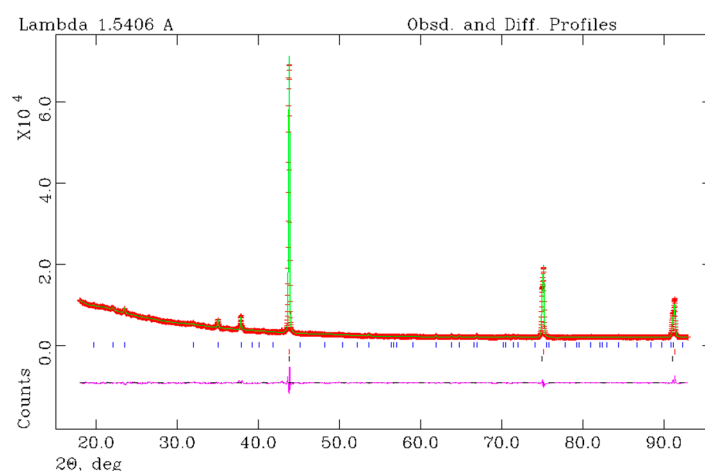

Figure 4. X-ray Rietveld refinement of the sample N1. The observed (+), calculated (solid line) and difference between observed and calculated (bottom curve) powder diffraction profiles. The positions of all allowed Bragg reflections are indicated by the rows of vertical tick marks: B_4C upper and diamonds lower marks.
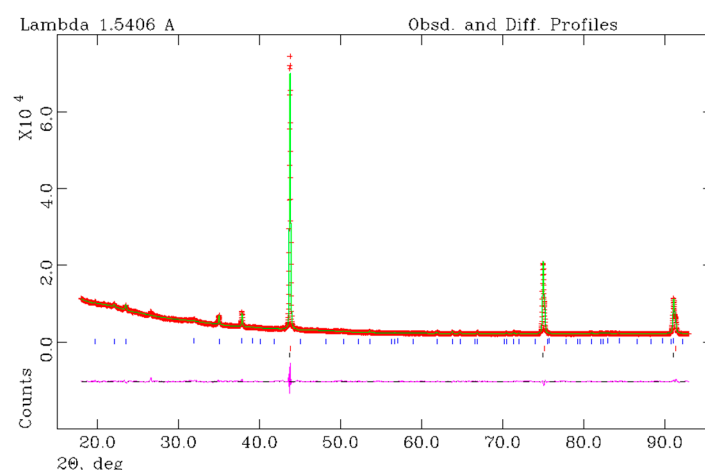

Figure 5. X-ray Rietveld refinement of the sample N2. The observed (+), calculated (solid line) and difference between observed and calculated (bottom curve) powder diffraction profiles. The positions of all allowed Bragg reflections are indicated by the rows of vertical tick marks: B_4C upper and diamonds lower marks.

Table 1. Experimental details for D1, D2, and B_4C (sample N1).

Chemical Formula	C (D1)	C (D2)	B_4C
Chemical formula weight	12.01	12.01	164.74
Space group	$Fd-3m$	$Fd-3m$	$R-3m$
a (Å)	3.57831(1)	3.57141(1)	5.5862(1)
b (Å)			5.5862(1)
c (Å)			12.0484(4)
γ (°)			120.00
V (Å^3)	45.818(0)	45.553(0)	325.611(13)
Z	8	8	3
D_x (Mg m^{-3})	3.266	3.388	2.506
Weight fraction, %	34.44(10)	54.51(5)	11.05(7)
Radiation type		Cu Kα_1	
Wavelength (Å)		1.5405981	
Temperature (K)		293	
Data collection			
Diffractometer	Imaging Plate Guinier camera G670, Huber		
Refinement	GSAS		
R_F	0.0091	0.0164	
R_P		0.0184	
R_{WP}		0.0276	

Table 2. Experimental details for D1, D2, and B_4C (sample N2).

Chemical Formula	C (D1)	C (D2)	B_4C
Chemical formula weight	12.01	12.01	164.74
Space group	$Fd-3m$	$Fd-3m$	$R-3m$
a (Å)	3.57708(1)	3.57010(2)	5.58783(9)
b (Å)			5.58783(9)
c (Å)			12.0477(3)
γ (°)			120.00
V (Å^3)	45.770(0)	45.503(1)	325.78(1)
Z	8	8	3
D_x (Mg m^{-3})	3.382	3.488	2.505
Weight fraction, %	66.51(4)	21.90(11)	11.59(7)
Radiation type		Cu Kα_1	
Wavelength (Å)		1.5405981	
Temperature (K)		293	
Data collection			
Diffractometer	Imaging Plate Guinier camera G670, Huber		
Refinement	GSAS		
R_F	0.0098	0.0138	
R_P		0.0175	
R_{WP}		0.0250	

The conducted refinement of the occupancy of carbon positions by boron in the Sample 1 gave a boron concentration of 29.8(8)% in D1 and 13.5(8)% in D2, which is higher than the calculated values. Similar values were obtained for Sample 2. This result clearly shows the deficiency of an electron density in the carbon positions. It can only be explained by the presence of vacancies since boron reduces the electron density by only one electron compared to the density on carbon, and a vacancy reduces it by six electrons. Table 3 shows the results of the refinement under the assumption that both boron atoms and vacancies are present in diamonds. In the refinement, the boron concentration was fixed: 3.12% for D1 and 1.56% for D2, which corresponded to the final total of 1.93% (it was assumed that the concentration of boron in D1 is two times higher than that in D2).

Table 3. Fractional atomic coordinates, site occupancy, and isotropic displacement parameters U_{iso} (Å^2) for D1 and D2 (Sample 1).

Phase	ATOM	Site	OCC	x	y	z	U_{iso}
D1	C	(8a)	0.910(3)	0.125	0.125	0.125	0.0166(1)
	B	(8a)	0.0312	0.125	0.125	0.125	0.0166(1)
D2	C	(8a)	0.953(3)	0.125	0.125	0.125	0.0141(1)
	B	(8a)	0.0156	0.125	0.125	0.125	0.0141(1)

4. Discussion

Table 3 shows that the concentration of vacancies in D1 is approximately 6%, while this is 3% in D2. This essentially means that each boron atom is associated with two vacancies in both diamonds. The same refinement for Sample 2 gives around three vacancies per B atom in both diamonds. It should be noted that we have prepared about 10 samples under different P–T conditions and different starting mixtures. The unit cell parameters of the obtained diamonds were either about 3.570 Å or 3.578 Å. Two different concentrations of boron can be associated with the presence of stable electronic states: semiconducting and metallic. In this case, the transition between states can be considered as an electronic Mott transition.

The refinement of the structure does not provide the reason for the discretization of the unit cell parameter of the diamonds although this shows the significant influence of vacancies as their concentration is 2–3 times higher than the boron concentration.

5. Conclusions

For the first time, by using Rietveld full-profile refinement, it is shown that the unit cell parameter of a diamond with boron has two discrete values: around 3.570 Å for small concentrations of B (~1–1.5%) or around 3.578 Å for large concentrations of B (~2–3%). It is also shown that these processes can be influenced by vacancies, the concentration of which is 2–3 times higher than the concentration of boron in diamonds.

Conflicts of Interest: The authors declare no conflicts of interest.

References

1. Scott, D.E. The history and impact of synthetic diamond cutters and diamond enhanced inserts on the oil and gas industry. *Ind. Diamond Rev.* **2006**, *1*, 48–58.
2. Vavilov, V.S. Diamond in solid state electronics. *Phys. Uspekhi* **1997**, *1*, 15–20. [CrossRef]
3. Nadolinny, V.; Komarovskikh, A.; Palyanov, Y. Incorporation of large impurity atoms into the diamond crystal lattice: EPR of split-vacancy defects in diamond. *Crystals* **2017**, *7*, 237. [CrossRef]
4. Ekimov, E.A.; Lyapin, S.G.; Boldyrev, K.N.; Kondrin, M.V.; Khmelnitskiy, R.; Gavva, V.A.; Kotereva, T.V.; Popova, M.N. Germanium–vacancy color center in isotopically enriched diamonds synthesized at high pressures. *JETP Lett.* **2015**, *102*, 701–706. [CrossRef]
5. Blank, V.D.; Kuznetsov, M.S.; Nosukhin, S.A.; Terentiev, S.A.; Denisov, V.N. The influence of crystallization temperature and boron concentration in growth environment on its distribution in growth sectors of type IIb diamond. *Diam. Relat. Mater.* **2007**, *16*, 800–804. [CrossRef]

6. Issaoui, R.; Achard, J.; Silva, F.; Tallaire, A.; Tardieu, A.; Gicquel, A.; Pinault, M.A.; Jomard, F. Growth of thick heavily boron-doped diamond single crystals: Effect of microwave power density. *Appl. Phys. Lett.* **2010**, *97*, 182101. [CrossRef]

7. Bautze, T.; Mandal, S.; Williams, O.A.; Rodiere, P.; Meunier, T.; Bauerle, C. Superconducting nano-mechanical diamond resonators. *Carbon* **2014**, *72*, 100–105. [CrossRef]

8. Tago, S.; Ochiai, T.; Suzuki, S.; Hayashi, M.; Kondo, T.; Fujishima, A. Flexible boron-doped diamond (bdd) electrodes for plant monitoring. *Sensors* **2017**, *17*, 1638. [CrossRef] [PubMed]

9. Ochiai, T.; Tago, S.; Hayashi, M.; Hirota, K.; Kondo, T.; Satomura, K.; Fujishima, A. Boron-doped diamond powder (BDDP)-based polymer composites for dental treatment using flexible pinpoint electrolysis unit. *Electrochem. Commun.* **2016**, *68*, 49–53. [CrossRef]

10. Ekimov, E.A.; Sidorov, V.A.; Bauer, E.D.; Melnik, N.N.; Curro, N.J.; Thompson, J.D.; Stishov, S.M. Superconductivity in diamond. *Nature* **2004**, *428*, 542–545. [CrossRef] [PubMed]

11. Dubrovinskaia, N.; Eska, G.; Sheshin, G.A.; Braun, H. Superconductivity in polycrystalline boron-doped diamond synthesized at 20 GPa and 2700 K. *J. Appl. Phys.* **2006**, *99*, 033903. [CrossRef]

12. Ekimov, E.A.; Ralchenko, V.; Popovich, A. Synthesis of superconducting boron-doped diamond compacts with high elastic moduli and thermal stability. *Diamond Relat. Mat.* **2014**, *50*, 15–19. [CrossRef]

13. Filonenko, V.P.; Zibrov, I.P. High-pressure phase transitions of M_2O_5 (M=V, Nb, Ta) and thermal stability of new polymorphs. *Inorg. Mater.* **2001**, *37*, 953–959. [CrossRef]

14. Zibrov, I.P.; Filonenko, V.P.; Werner, P.-E.; Marinder, B.-O.; Sundberg, M. A new high-pressure modification of Nb_2O_5. *J. Solid State Chem.* **1998**, *141*, 205–211. [CrossRef]

15. Szirmai, P.; Pichler1, T.; Williams, O.A.; Mandal, S.; Bäuerle, C.; Simon, F. A detailed analysis of the Raman spectra in superconducting boron doped nanocrystalline diamond. *Phys. Status Solidi B* **2012**, *249*, 2656–2659. [CrossRef]

16. Larson, A.C.; Von Dreele, R.B. *General Structure Analysis System (GSAS)*; Report LA-UR-86-748; Los Alamos National Laboratory: Los Alamos, NM, USA, 1987.

17. Toby, B.H. EXPGUI, a graphical user interface for GSAS. *J. Appl. Crystallogr.* **2001**, *34*, 210–213. [CrossRef]

18. Kwei, G.H.; Morosin, B. Structures of the boron-rich boron carbides from neutron powder diffraction: Implications for the nature of the inter-icosahedral chains. *J. Phys. Chem.* **1996**, *100*, 8031–8039. [CrossRef]

19. Ponomarev, V.I.; Kovalev, I.D.; Konovalikhin, S.V.; Vershinnikov, V.I. Ordering of Carbon atoms in boron carbide structure. *Cryst. Rep.* **2013**, *58*, 422–427. [CrossRef]